ISSN (Print) : 2320 – 3765
ISSN (Online): 2278 – 8875

International Journal of Advanced Research in Electrical, Electronics and Instrumentation Engineering

(An ISO 3297: 2007 Certified Organization)

Volume 4, Issue 3, March 2015

A Hardware Implementation of Bridgeless Boost Converter for Low Power Application

M.Vimal kumar[1], K.Nandakumar[2], R.Anandaraj[3]

PG Scholar [PED], Dept. of EEE, E.G.S.Pillay Engineering College, Nagapattinam, Tamilnadu, India[1]

Assistant Professor, Dept. of EEE, E.G.S.Pillay Engineering College, Nagapattinam, Tamilnadu, India[2]

Head of the Department, Dept. of EEE, E.G.S.Pillay Engineering College, Nagapattinam, Tamilnadu, India[3]

ABSTRACT: In this paper, a single-stage ac–dc power electronic converter is proposed to efficiently manage the energy harvested from electromagnetic microscale and mesoscale generators with low-voltage outputs. The proposed topology combines a boost converter and a buck-boost converter to condition the positive and negative half portions of the input ac voltage respectively. Only one inductor and capacitor are used in both circuitries to reduce the size of the converter. A 2 cm × 2 cm, 3.34-g prototype has been designed and tested at 50-kHz switching frequency, which demonstrate 71% efficiency at 54.5 mW. The input ac voltage with 0.4 V amplitude is rectified and stepped up to 3.3 V dc. Detailed design guidelines are provided with the purpose of minimizing the size, weight, and power losses. The theoretical analyses are validated by the experiment results.

I. INTRODUCTION

Kinetic energy harvesters convert mechanical energy present in the environment into electrical energy. The past decade has seen an increasing focus in the research community on kinetic energy harvesting devices. Typically, kinetic energy is converted into electrical energy using electromagnetic, piezoelectric, or electrostatic transduction mechanisms. In comparison to electrostatic and piezoelectric transducers, electromagnetic transducers outperform in terms of efficiency and power density. In this study, electromagnetic energy harvesters are considered for further study.

A general diagram of an electromagnetic generator is demonstrated in Fig. 1, where *k* is spring stiffness constant; *m* is the proof-mass; *DE* and *DP* represent electrical and parasitic dampers, respectively. Essentially, the energy harvesting system consists of a spring, a proof mass, and an electrical damper. The extrinsic vibrations excite the internal oscillation between the proof mass (magnet) and electrical damper (coils). The internal oscillation produces a periodically variable magnetic flux in the coil, which induces a corresponding alternating output voltage.

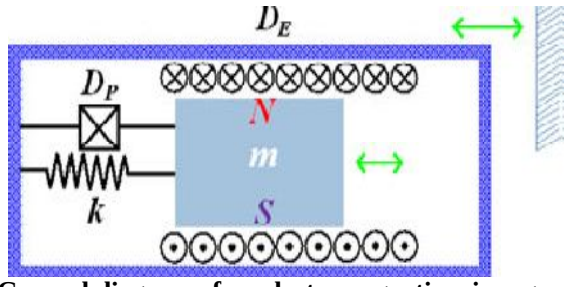

Fig.1. General diagram of an electromagnetic micro generator.

In energy harvesting systems, power electronic circuit forms the key interface between transducer and electronic load, which might include a battery. The electrical and physical characteristics of the power conditioning interfaces determine the functionality, efficiency and the size of the integrated systems. The power electronic circuits are employed to 1) regulate the power delivered to the load and 2) actively manage the electrical damping of the transducers so that maximum power could be transferred to the load. The output voltage level of the microscale and mesoscale energy harvesting devices is usually in the order of a few hundred milli volts depending on the topology of device. The output ac voltage should be rectified, boosted, and regulated by power converters to fulfill the voltage

ISSN (Print) : 2320 – 3765
ISSN (Online): 2278 – 8875

International Journal of Advanced Research in Electrical, Electronics and Instrumentation Engineering

(An ISO 3297: 2007 Certified Organization)

Volume 4, Issue 3, March 2015

requirement of the loads. Nonetheless, miniature energy harvesting systems have rigid requirement on the size and weight of power electronic interfaces.

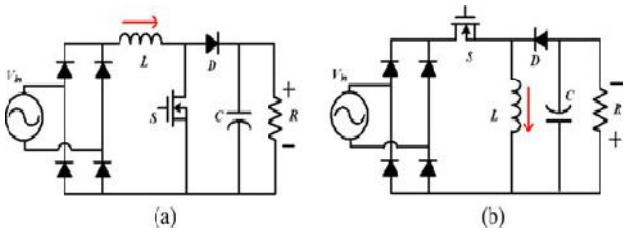

Fig.2. Conventional two-stage diode-bridge ac–dc converters (a) Boost rectifier (b) Buck-boost rectifier

Conventional ac–dc converters for energy harvesting and conditioning usually consists of two stages. A diode bridge rectifier typically forms the first stage, while the second stage is a dc–dc converter to regulate the rectified ac voltage to a dc voltage (see Fig. 2). However, the diode bridge would incur considerable voltage drop, making the low-voltage rectification infeasible.

To overcome these drawbacks, CMOS diodes with low voltage drops are investigated in the bridge rectifiers, to substitute conventional p-n junction diodes. Such reported diodes include 1) diode-connected passive MOSFET, which adopts threshold voltage cancellation techniques and 2) MOSFET, which is actively controlled by a comparator. In either case, the low-voltage-drop diode techniques require either additional bias networks or external comparators. Thus, both the complexity and the power loss of the circuitry would increase. Some converters reported in the literature use transformers as the first stage boosters to overcome the voltage drop in semiconductor devices. However, the size of the transformer could be unacceptably large in low-frequency energy harvesting applications.

Another approach to maximize the conversion efficiency in low-voltage rectification is to use bridgeless direct ac–dc converters. Those topologies either use bidirectional switches and split capacitors, or two parallel dc–dc converters to condition positive and negative input voltages separately. For the split-capacitor topologies [see Fig. 3(a)–(c)], due to the low operation frequency of specified micro generators, the capacitors have to be large enough to suppress the voltage ripple under a desired level.

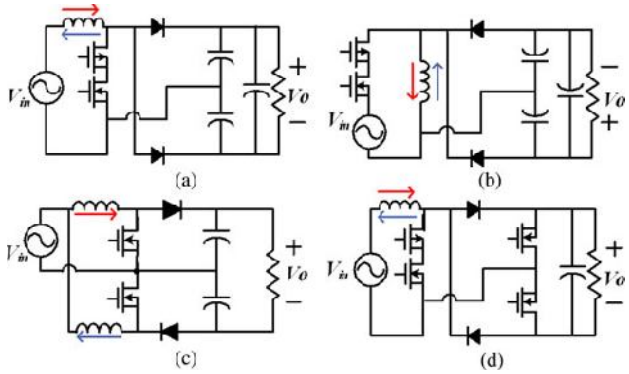

Fig. 3. Bridgeless ac–dc converters [6]

(a) Split capacitor boost converter
(b) Split capacitor buck-boost converter
(c) Dual polarity boost converter
(d) Boost converter with secondary switches

The increased size and number of energy storage components make those topologies impractical due to the size limitation of energy harvesters. On the other hand, the split capacitors could be eliminated by using two

ISSN (Print) : 2320 – 3765
ISSN (Online): 2278 – 8875

International Journal of Advanced Research in Electrical, Electronics and Instrumentation Engineering

(An ISO 3297: 2007 Certified Organization)

Volume 4, Issue 3, March 2015

synchronous MOSFETs [see Fig. 3(d)]. However, the additional switches would incur extra switch loss and driving circuit dissipations.

The boost converter is the common power conditioning interface due to its simple structure, voltage step-up capability and high efficiency. The buck-boost converter has ability to step up the input voltage with a reverse polarity; hence, it is an appropriate candidate to condition the negative voltage cycle. Besides, the boost and buck-boost topologies could share the same inductor and capacitor to meet the miniature size and weight requirements.

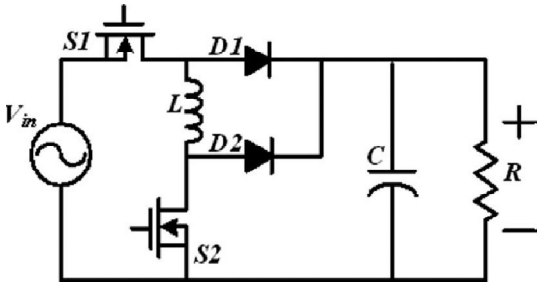

Fig. 4. Proposed bridgeless boost rectifier for low-voltage energy harvesting

A new bridgeless boost rectifier, shown in Fig. 4, which is a unique integration of boost and buck-boost converters, is proposed in this paper. When the input voltage is positive, *S*1 is turned ON and *D*1 is reverse biased, the circuitry operates in the boost mode. As soon as the input voltage becomes negative, the buck-boost mode starts with turning ON *S*2 and reverse biasing *D*2. MOSFETs with bidirectional conduction capability work as two-quadrant switches to ensure the circuitry functionality in both positive and negative voltage cycles. This topology was introduced for piezoelectric energy harvesting applications.

The circuit operation modes are described in Section II. Section III addresses the control schemes for DCM. Experiment results are reported to verify the previous theoretical analysis in Section IV. Section V presents the conclusions.

II. PRINCIPLE OF OPERATION

In electromagnetic energy harvesters, the internal oscillation between coils and magnet produces a periodically variable magnetic flux in the coil, which induces a corresponding output voltage. The power electronics interface (PEI) is employed to supply constant voltage and to deliver power to the load. In order to facilitate and simplify analyses, it is assumed that the input impedance of the PEI is significantly larger than the internal impedance of energy harvesting device. The induced voltage could be assumed to be a low amplitude sinusoidal ac voltage source. As the frequency of vibration source and induced voltage (usually less than 100 Hz) is much less in comparison to that of the switching frequency (around tens of kHz), the induced ac voltage can be assumed as a constant voltage source in each switching period. In this paper, a 0.4 V, 100 Hz sinusoidal ac voltage source is adopted to emulate the output of the electromagnetic energy harvester.

The DCM operating modes of the proposed boost rectifier are shown in Fig. 5. Each cycle of the input ac voltage can be divided into six operation modes. Modes I–III illustrate the circuit operation during positive input cycle, where *S*1 is turned ON while *D*1 is reverse biased. The converter operates as a boost circuit during Modes I–III, while switching *S*2 and *D*2. The operation during negative input cycle is demonstrated in Modes IV–VI, where *S*2 is turned ON while *D*2 is reverse biased. In these modes, the converter operates similar to a buck-boost circuit.

Mode I: This mode begins when *S*2 is turned ON at t_0. The inductor current is zero at t_0. The turn on of *S2* is achieved through zero current switching (ZCS) to reduce switching loss. Inductor *L* is energized by the input voltage as both *S*1 and *S*2 are conducting. Both diodes are reverse biased. The load is powered by the energy stored in the output filter capacitor *C*.

ISSN (Print) : 2320 – 3765
ISSN (Online): 2278 – 8875

International Journal of Advanced Research in Electrical, Electronics and Instrumentation Engineering

(An ISO 3297: 2007 Certified Organization)

Volume 4, Issue 3, March 2015

Mode II: $S2$ is turned OFF at t_1, where $t_1 - t_0 = d_1 Ts$, d_1 is the duty cycle of the boost operation, and T_s is the switching period. The energy stored in the inductor during Mode I is transferred to the load. The inductor current decreases linearly. During this mode, switching loss occurs during the turn on of diode $D2$.

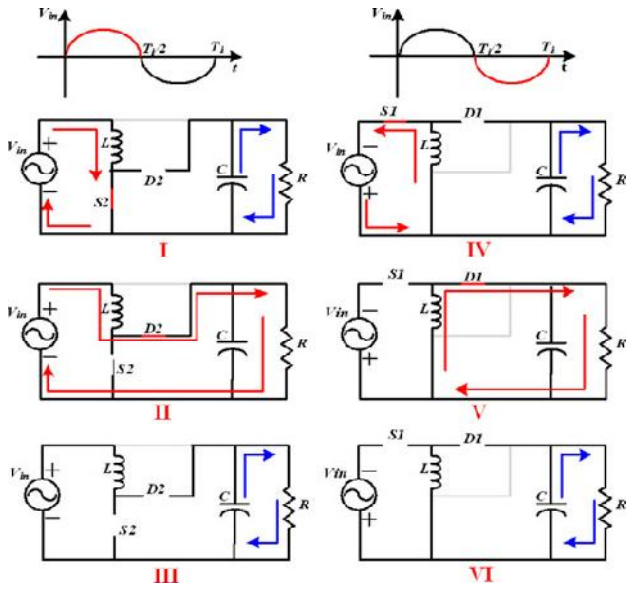

Fig. 5. Operating modes of the proposed boost rectifier

Mode III: $D2$ is automatically turned OFF as soon as the inductor current becomes zero at t_2 ($t_2 - t_1 = d_2 T_s$). This avoids the reverse recovery loss of diode. The load is again powered by the stored energy in the capacitor. The converter would return to Mode I as soon as $S2$ is turned ON, if the input voltage is still in positive cycle.

Mode IV: During the negative input cycle, Mode IV starts as soon as $S1$ is turned ON at t'_0. ZCS condition can also be achieved by ensuring the converter operation in DCM. The energy is transferred to the inductor L again, while the output filter capacitor C feeds the load.

Mode V: At t'_1, $S1$ is turned OFF, where $t'_1 - t'_0 = d'_1 T_s$, d'_1 is the duty cycle of the buck-boost operation. The energy stored in the inductor during Mode IV is transferred to the load. The inductor current decreases linearly. During this mode, switching loss occurs during the turn on of the diode $D1$.

Mode VI: When the inductor current decreases to zero at t'_2 ($t'2 - t'_1 = d'_2 T_s$), $D1$ is turned OFF at zero current. The load is continuously powered by the charge stored in the output capacitor. The converter would return to Mode IV as soon as $S1$ is turned ON, if the input voltage is still negative.

ISSN (Print) : 2320 – 3765
ISSN (Online): 2278 – 8875

International Journal of Advanced Research in Electrical, Electronics and Instrumentation Engineering

(An ISO 3297: 2007 Certified Organization)

Volume 4, Issue 3, March 2015

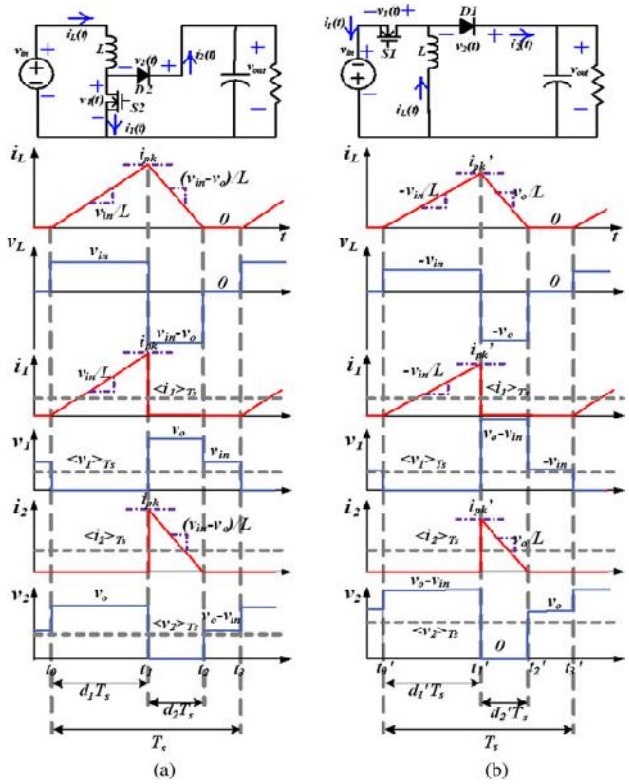

Fig. 6. Waveforms of the proposed boost/buck-boost rectifier (a) Boost operation (b) Buck-boost operation

According to the analyses of operation modes, the switches are turned ON with ZCS and the diodes are turned OFF with ZCS. Due to the DCM operation, the input current sensor can be eliminated and switching loss can be reduced. Moreover, the control scheme of DCM operation is relatively simpler. Since the circuit size can be reduced and the efficiency can be enhanced, DCM operation is more suitable than continuous conduction mode (CCM) operation.

III. CONTROL STRATEGY

For a dynamic EM energy harvester system, if the external excitation frequency is different from the intrinsic resonance frequency, the PEI should be able to match its input impedance with the internal impedance of the harvester so that maximum power point (MPP) could be tracked. This paper proposed a new topology, which has the maximum power point tracking (MPPT) capability. However, the main objective of this paper is to introduce the circuit topology, which is capable of satisfying the voltage requirement (3.3 V) of an electronic load. Thus, a voltage feedback control loop is utilized to regulate the load voltage.

The simplified scheme of the controller and power stage is illustrated in Fig. 7. The converter is designed to operate in DCM. The output voltage is filtered by a passive low-pass filter and then fed to the analog-to-digital converter (ADC) of the controller.

ISSN (Print) : 2320 – 3765
ISSN (Online): 2278 – 8875

International Journal of Advanced Research in Electrical, Electronics and Instrumentation Engineering

(An ISO 3297: 2007 Certified Organization)

Volume 4, Issue 3, March 2015

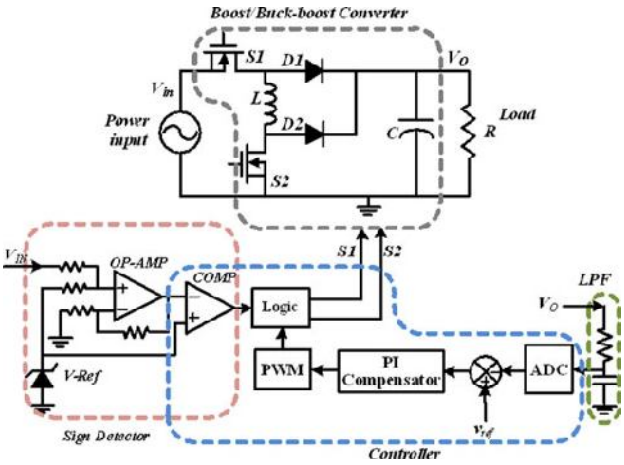

Fig. 7. Control circuit for the proposed converter

The difference between the ADC output and the desired voltage is calculated and compensated through the PI algorithm to generate an adjustable duty cycle signal. The switching signals of *S*1 and *S*2 are dependent on the polarity of the input voltage. A sign detector is used to determine the input voltage polarity. The Atmel Mega 16 A is selected as the controller in this paper, which has both on-chip analog comparator and integrated ADC and can be integrated with the sign detector.

The sign detector is composed of a voltage reference, an op-amp, and the on-chip analog comparator. The op-amp operates as an analog adder, where a dc bias (voltage reference) is added to the input voltage. The signal summation is compared with the voltage reference to detect the polarity.

IV. EXPERIMENT RESULTS AND LOSS ANALYSES

The printed circuit board (PCB) is designed to minimize the size of the prototype using surface-mount components with lower packaging overhead. In the case of much lower power levels, it is possible to use components with least packaging overhead or in bare die form to further reduce the size and weight of the circuit. A highly compact power electronic interface prototype, depicted in Fig. 8 is fabricated. The prototype has a PCB size of 2 × 2 cm^2 and weighs 3.34 g. The component design details and electrical parameters are summarized in Table I.

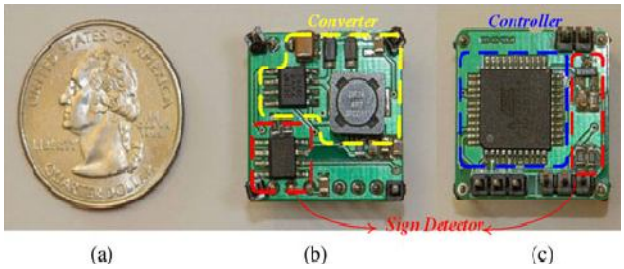

Fig.8. 2 × 2 cm^2 , 3.34 g prototype of the proposed converter (a) United States quarter (b) Circuit Front (c) Circuit Back

*S*2 operates as the low-side switch with *V*GS2 = *VG*2, while *S*1 operates as the high-side switch with *V*GS1 = *VG*1 − *V*in. In this case, due to small amplitude of input voltage, the minimum value of *V*GS1 = *VG*1−*VM* = 2.9 V is still sufficient to turn on the *S*1 with low conduction resistance. Thus, both *S*1 and *S*2 could be directly driven by the digital output of the controller.

ISSN (Print) : 2320 – 3765
ISSN (Online): 2278 – 8875

International Journal of Advanced Research in Electrical, Electronics and Instrumentation Engineering

(An ISO 3297: 2007 Certified Organization)

Volume 4, Issue 3, March 2015

The energy harvester is emulated by a signal generator cascaded with a high-pass filter, and a high current voltage follower (OPA548). The power source is programmed to have 0.4-V amplitude and 100-Hz frequency.

A milliwatt scale test is carried out in order to verify the theoretical analyses and simulations of the proposed topology. However, this proposed topology is not specifically limited to be used in milliwatt applications; it would also work in microwatt applications.

TABLE I
COMPONENTS AND PARAMETERS IN THE PROTOTYPE

COMPONENT	PARAMETERS	Part Number
V_{in} (Input voltage)	0.4 V, 100 Hz	N/A
V_o (output voltage)	3.3 V	N/A
Switching frequency	50 kHz	N/A
Power Inductor L	4.7 μH, 3.34 A, 25.4 mΩ	DR74-4R7-R
Filter Capacitor C	100 μF, 6.3 V	C3225Y5V0J107Z
MOSFETs	20 V, 8 A, 22 mΩ@2.5 V	SI9926CDY
Schottky Diodes	20 V, 0.36 V@1 A	DFLS120L-7

200Ωresistive load is chosen to demonstrate the power transfer capability of the designed PEI prototype. With 200Ω resistive load, the converter is capable of tightly regulating output voltage and delivering 54.5 mW to the load. Figs. 9–12 illustrate the experimental waveforms for the converter with a 200-Ω resistive load. Fig. 9 shows the waveforms of input voltage, gate signals of both switches, as well as the input current. During the positive input cycle, *S*1 is turned ON, while *S*2 is driven by the boost control scheme. When the circuit operates in the negative input cycle, *S*2 is turned ON, while *S*1 is controlled under the buck-boost conditioning strategy. As seen from Fig. 10, the output voltage is regulated at 3.3V dc with approximately 0.2V (i.e., 6%) voltage ripple.

Fig. 11 and 12 demonstrate the boost and buck-boost operations correspondingly. Closed-loop voltage control successfully stabilizes the duty cycle at 0.72 at the steady state. In boost operation, the input current increases with a rate of 33.3 mA/μs, and then drops fast with a rate of 200 mA/μs. The discontinuous condition lasts approximately 8 μs during each cycle. In buck-boost operation, the input current becomes zero as soon as *S*1 is switched OFF.

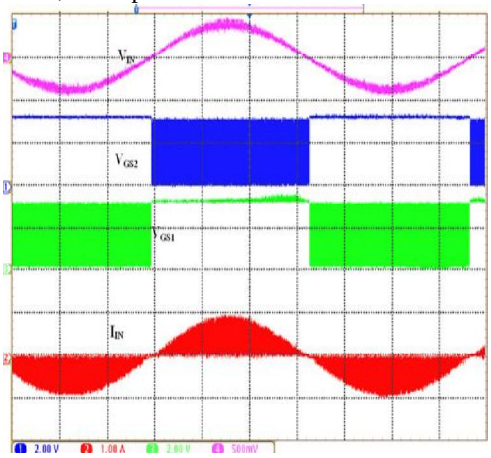

Fig. 9. ***From top to bottom:*** **oscillograms of input voltage (0.5 V/div), boost gate pulse (2 V/div), buck-boost gate pulse (2 V/div), input current (1 A/div); time 4 ms/div, R = 200 Ω**

ISSN (Print) : 2320 – 3765
ISSN (Online): 2278 – 8875

International Journal of Advanced Research in Electrical, Electronics and Instrumentation Engineering

(An ISO 3297: 2007 Certified Organization)

Volume 4, Issue 3, March 2015

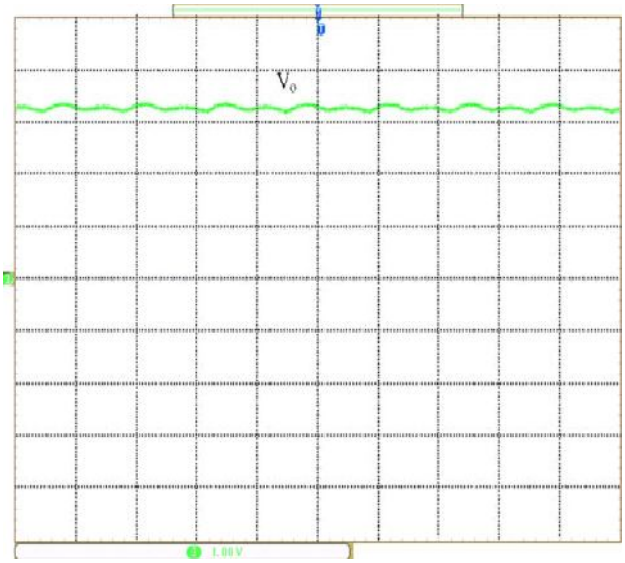

Fig. 10. Oscillogram of output voltage, 1 V/div; time 20 ms/div. *R* = 200 Ω.

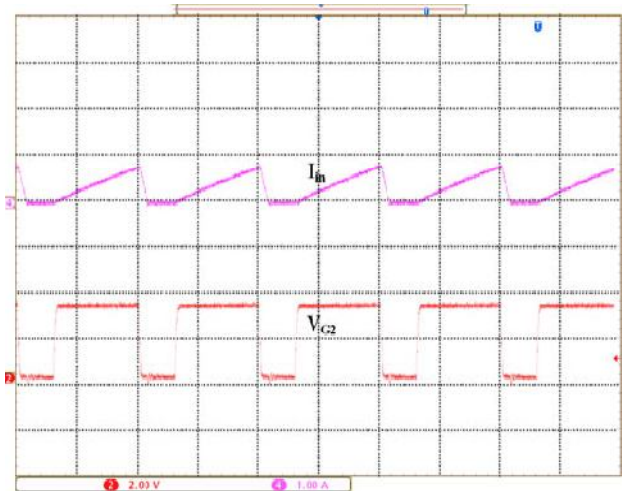

Fig. 11. *From top to bottom:* oscillograms of input current (500 mA/div), boost gate pulse (2 V/div); time 10 *μ*s/div. *R* = 200 Ω

ISSN (Print) : 2320 – 3765
ISSN (Online): 2278 – 8875

International Journal of Advanced Research in Electrical, Electronics and Instrumentation Engineering

(An ISO 3297: 2007 Certified Organization)

Volume 4, Issue 3, March 2015

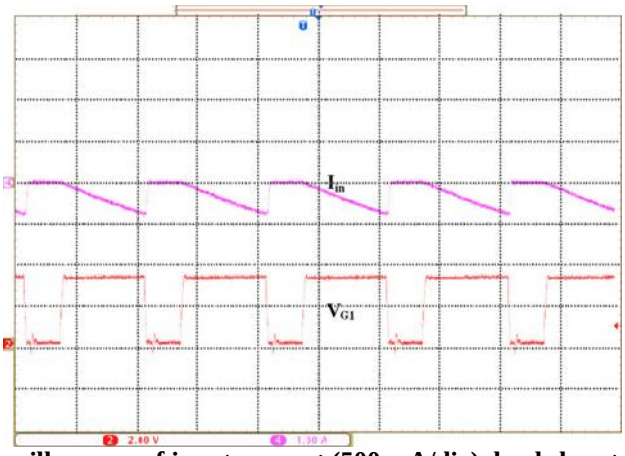

Fig. 12. ***From top to bottom:*** **oscillograms of input current (500 mA/div), buck-boost gate pulse (2 V/div); time 10 μs/div. R = 200 Ω**

TABLE II
COMPARISONS ON CALCULATED AND MEASURED PARAMETERS

Parameter	Calculated Value	Measured Value
Duty cycle (R= 200 Ω)	0.65	0.72
$\Delta I_{in,max}$ (R = 200 Ω)	1.1 A	1.02A
Duty cycle (R = 300 Ω)	0.56	0.60
$\Delta I_{in,max}$ (R = 300 Ω)	0.95 A	0.84 A

The conduction losses and switching losses of both active and passive components are estimated according to the experiment data and the parasitic parameters offered in Table I. Due to ZCS operation, the switching losses are minimized. The conduction loss dominates in the total conversion losses. Both the quiescent and dynamic losses of each IC are also estimated according to the provided corresponding data sheet. The estimated losses of individual component are listed in Table III, under 200-Ω resistive load condition. A 71% conversion efficiency is measured from experiment, which is higher than the state of the art rectifiers for low-voltage applications (61%).

TABLE III
LOSS CALCULATION

Category	Component	Estimated Loss
Topology	Inductor	5.7 mW
	Filter Capacitor	0.06 mW
	MOSFETs	5.6 mW
	Diodes	6.3 mW
Controller	Mega 16A	1.98 mW
Sign Detector	Voltage Reference	0.33 mW
	OP-AMP	0.08 mW
Others	Trace and Contact resistances	2.0 mW
	Total Loss	22.05 mW

ISSN (Print) : 2320 – 3765
ISSN (Online): 2278 – 8875

International Journal of Advanced Research in Electrical, Electronics and Instrumentation Engineering

(An ISO 3297: 2007 Certified Organization)

Volume 4, Issue 3, March 2015

V. CONCLUSION

A single stage ac-dc topology for low-voltage low-power energy harvesting applications is proposed in this paper. The topology uniquely combines a boost converter and a buck-boost converter to condition the positive input cycles and negative input cycles, respectively. Only one inductor and one filter capacitor are required in this topology. A compact 2 cm×2 cm, 3.34 g prototype is fabricated and tested at 54.5 mW. This prototype successfully boosts the 0.4-V, 100-Hz ac to 3.3-V dc. Output voltage is tightly regulated at 3.3 V through closed-loop voltage control. The measured conversion efficiency is 71% at 54.5mW. In comparison to state-of-the-art low-voltage bridgeless rectifiers, this study employs the minimum number of passive energy storage components, and achieves the maximum conversion efficiency. The future research will be focused on investigating and designing integrated three-phase power electronic interfaces for electromagnetic energy harvesting.

REFERENCES

[1] S. Roundy, P. K. Wright, and J. Rabaey, "A study of low level vibrations as a power source for wireless sensor nodes," *Comput. Commun.*, vol. 26, no. 11, pp. 1131–1144, Jul. 2003.
[2] M. El-hami, P. Glynne-Jones, N. M. White, M. Hill, S. Beeby, E. James, A. D. Brown, and J. N. Ross, "Design and fabrication of a new vibration based electromechanical power generator," *Sens. Actuators A: Phys.*, vol. 92, no. 1–3, pp. 335–342, Aug. 2001.
[3] S. P. Beeby, R. N. Torah, M. J. Tudor, P. Glynne-Jones, T. O'Donnell, C. R. Saha, and S. Roy, "A micro electromagnetic generator for vibration energy harvesting," *J. Micromech. Microeng.*, vol. 17, no. 7, pp. 1257–1265, Jul. 2007.
[4] R. Vullers, R. van Schaijk, and I. Doms, "Micropower energy harvesting,"*Solid-State Electron.*, vol. 53, no. 7, pp. 684–693, Jul. 2009.
[5] C. B.Williams, C. Shearwood, M. A. Harradine, P. H.Mellor, T. S. Birch, and R. B. Yates, "Development of an electromagnetic micro-generator," *IEE Proc. Circuits Devices Syst.*, vol. 148, no. 6, pp. 337–342, Jun. 2001.
[6] G. D. Szarka, B. H. Stark, and S. G. Burrow, "Review of power conditioning for kinetic energy harvesting systems," *IEEE Trans. Power Electron.*, vol. 27, no. 2, pp. 803–815, Feb. 2012.
[7] S. G. Burrow and L. R. Clare, "Open-loop power conditioning for vibration energy harvesters," *Electron. Lett.*, vol. 45, no. 19, pp. 999–1000, Sep. 2009.
[8] Cammarano, S. G. Burrow, D. A. W. Barton, A. Carrella, and L. R. Clare, "Tuning a resonant energy harvester using a generalized electrical load," *Smart Mater. Structures*, vol. 19, no. 5, pp. 1–7, May 2010.
[9] S. Cheng, N. Wang, and D. P. Arnold, "Modeling of magnetic vibrational energy harvesters using equivalent circuit representations," *J. Micromech. Microeng.*, vol. 17, no. 11, pp. 2328–2335, Nov. 2007.
[10] R. Dayal and L. Parsa, "A new single stage AC-DC converter for low voltage electromagnetic energy harvesting," in *Proc. IEEE Energy Convers. Congr. Expo.*, Atlanta, GA, USA, Sep. 2010, pp. 4447–4452.